Review _____ *Forma*, **21**, 67–80, 2006

Visualization of Forms in the Inside of the Human Body

Junichiro TORIWAKI

Department of Life System Science and Technology, Chukyo University, Toyota 470-0393, Japan
E-mail address: jtoriwak@life.chukyo-u.ac.jp

(Received February 26, 2005; Accepted July 4, 2005)

Keywords: Organs, Lung, Colon, Human Body, 3D CT Images, Virtual Endoscopy, Micro CT Images

Abstract. This article presents a brief review of methods to visualize forms of parts of the human body in different spatial resolutions by applying navigation observation and pattern recognition to three dimensional (3D) X-ray CT images. Several examples of 3D views of the parts of human body are shown. They are characterized by that the viewpoint is selected arbitrarily inside the body and moved around anywhere almost continuously.

1. Introduction

Human organs have very complicated form, sometimes far beyond our imagination. We need to know forms of various parts of organs and tissues as exactly as possible to diagnose diseases and treat them because some kinds of changes will be observed necessarily due to diseases. Apart from such medical requirements forms of human body or parts of it will be helpful to creative activity such as painting and sculpture, animation production, and industrial design

Recent development of technology has made it possible to see forms of various parts of human body without injuring it. In particular, imaging technologies such as CT and MRI in medicine contribute much (DUCHMAN, 2000). For instance, by 3D X-ray CT we can reconstruct parts of human body on computer memory with 0.5 mm^3 of spatial resolution. Molecular imaging provides a method to record functions and shapes of molecule level. By micro CT we can observe microstructure in the spatial resolution of micron-meter order (MATSUBARA *et al*., 2004; SATO *et al*., 2004).

In this article, the author presents a brief review of methods to visually observe or to visualize forms of parts of human body in different spatial resolutions by applying navigation observation and pattern recognition to three-dimensional (3D) X-ray CT images. We also show several examples of 3D views of the parts of human body. They are characterized by that the viewpoint is selected arbitrarily inside the body and moved around anywhere almost continuously.

By imaging technology, we obtain a 3-dimensinonal array recording the parts of the individual human body. This is regarded as a virtualized version of the individual human body. We call this *the virtualized human body* (VHB) (TORIWAKI, 1997). VHB is a replica

of the individual human body. However, we (human visual system) cannot see such a set of 3D numerical values directly. In order to visualize it we employ a CG technique known as the volume rendering (LEVOY, 1988; TORIWAKI, 2002). Visualization methods are more enriched by combining them with navigation and structurization.

2. Visualization of 3D Images

In the case of the observation of the human body, the original data is a set of three dimensional (3D) density values obtained by scanning human body by imaging equipments such as X-ray CT and MRI. We call this 3D array a *3D digital picture* (*image*) (TORIWAKI, 2002c). The 3D array of numerical data stores physical measurement data of 3D volume elements of the human body such as the attenuation factor of X-ray measured by scanners. The spatial resolution spreads over the range of 1 cm to 10 μm. However we cannot see directly the inside structure of such 3D array of numerical data unless utilizing visualization techniques.

The visualization technique that is employed most widely now is the volume rendering (VolR). We do not intend to explain details of VolR here. Details will be found in (TORIWAKI, 2002c; MORI *et al*., 2003), if necessary. Instead we will give brief comments to be noted in seeing images rendered with VolR below.

(1) VolR is considered as a kind of the orthogonal or the perspective mapping of a 3D array of numerical data (or a solid) to a 2D picture plane. Therefore a gray tone value (density value) on a resulting 2D picture is an accumulative sum or multiplication of density values of an original 3D picture along a line of mapping (called "*the ray*" in the field of computer graphics) (MORI *et al*., 2003) (Fig. 1).

(2) Before generating a VolR picture, we replace density values by suitable values, usually for the convenience of understanding spatial distribution of original density values by human vision. The resultant values of replacement are called "*opacity*". Correspondence relationship among density values and opacity values is defined by the *opacity table*, which

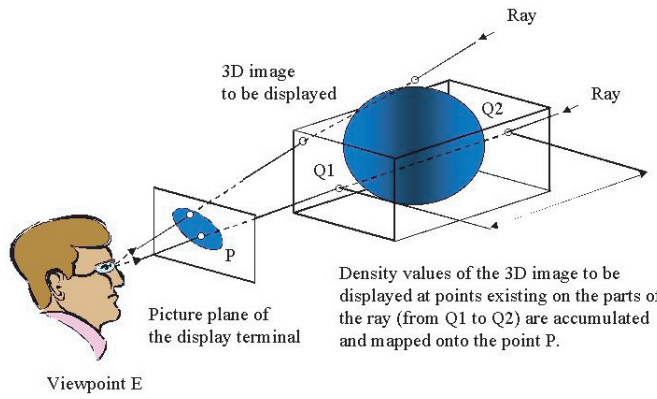

Fig. 1. Illustration of the volume rendering.

is most important parameters of VolR user can select.

(3) Voxels in a 3D picture may be divided into subgroups if possible, so that different colors may be assigned to each subgroup. By using colors we can attract observers' attention to particular objects in a displayed picture. Assignment of colors is defined by a *color table* in the VolR system, which is the other important parameter given by a user.

(4) If a solid object in a 3D space is defined explicitly, we can draw the surface of the solid object on a 2D display. This is done by another well known method of computer graphics "*surface rendering* (SurR)". We will neglect explanation of SurR here, because it is also found in any textbook of computer graphics easily (WATT and POLICARPO, 1998).

(5) From the viewpoint of shape understanding, VolR is considered as the method directed to discovering or finding form existing in natural phenomena or natural things without much a priori knowledge. As was introduced above, it contains two sets of parameters "*opacity table*" and "*color table*". Observed forms or resulting "impression" of generated images greatly depends on these two parameter sets.

(6) On the other hands, SurR is the method directed more strongly toward design or creation of a new form artificially. In order to apply SurR to natural objects such as the human body, we need to extract border surfaces of objects beforehand. To perform this automatically, pattern recognition of solid objects or border surfaces in 3D space is required (TORIWAKI, 2002c). Details of pattern recognition are omitted here because important parts of it have already been described in (TORIWAKI, 2002c)

3. Navigation

In the ordinary volume rendering, we assume a fixed viewpoint and fixed view directions. Also we set necessary parameters fixed such as opacity parameters. Although all of them may be given arbitrarily, they are fixed once they were given. In several applications, however, parts of viewing parameters (positions of viewpoints and view directions) may be changed interactively by users. In medical applications this technique is well known as virtual endoscopy nowadays (VINING *et al*., 1993; MORI *et al*., 1994; ROGALLA *et al*., 2000; VINING, 2003). Sometimes they are called by the name of the target organs to be diagnosed such as virtual colonoscopy and virtual bronchosccopy (ROGALLA, 2000; DUCHMAN, 2003).

Technically this is not difficult if recent computers with graphic engine are available. Let us represent a two dimensional (2D) picture sequence by $\mathbf{F} = \{F(t)\} = \{\{fij(t)\}\}$, where $fij(t)$ means a gray tone value at the i-th row and the j-th column at the time t. If we generate a 2D image $F(t)$ in the suitable rate, faster than 10 frames/sec, for example, with changing the location of the view point gradually we can produce a moving picture sequence which gives the impression that we fly through the inside of tublar organs such as colon. We call this way of presentation the navigation (TORIWAKI, 1997). The picture sequence $\mathbf{F}$ is a time sequence of 2D pictures $F(t)$, which shows a scene, seen when our viewpoint moves along the time axis. This is not the only possible way of the viewpoint movement. Conceptually various types of navigation along other axis will be considered. We call this the generalized navigation or navigation observation (TORIWAKI, 1997, 2004a, 2004b). One interesting example is the change in the physical scale, or the magnification. The example is found in (MORROSON, 1982).

In general, by seeing generated picture sequences we can get feeling that we are traveling inside the object or inside abstract space along a suitably defined axis. In this sense, virtual endoscope images show moving images which might be seen during driving cars or airplanes inside human body or flying though pipeline shape of organs along their inside wall with small airplanes. These feelings are aroused from the moving of a viewpoint along the real world coordinate axis. Conceptually the movement of the viewpoint along various other axes is considered, such as the physical scale, opacity, and time (TORIWAKI, 2004a).

4. Collective Examples of Inside Views of the Human Body

Let us show examples of pictures generated by rendering applying VolR and SurR to 3D CT images of real human body. They have been produced and collected in the process of researches in authors' group concerning computer aided diagnosis of cancer, pattern recognition of 3D images, computer graphics, and visualization of 3D gray tone images. We do not intend here to give accurate medical meanings to those images. Instead we expect readers to enjoy views inside human body. Also they could find how complicated forms exist inside our body that is usually invisible.

4.1. Example 1: The inside view of colon

The first image is the view of the colon (HAYASHI *et al*., 2003a, b; ODA *et al*., 2004; KITASAKA *et al*., 2004). Figure 2 shows the outside view of colon. Blue curves show approximated center lines automatically determined by a 3D thinning algorithm (SAITO and TORIWAKI, 1994, 1995; TORIWAKI and MORI, 2001). If observer's viewpoint proceeds into the colon along these centerlines, the observer can see scenes of the space inside colon. Let us show in Fig. 3 an example of a picture sequence, which is consisting of successive scenes obtained by virtual colonoscopy. The colon wall has many successive convex and concave parts called "haustra" in medicine. By presenting each scene with the enough high

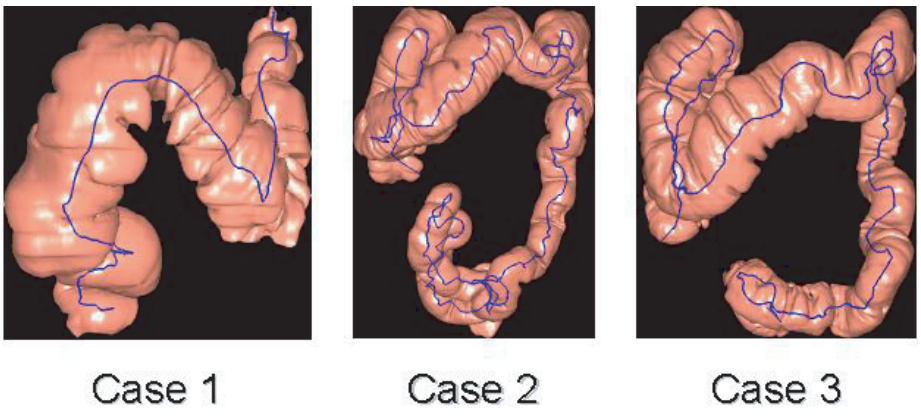

Fig. 2. The outside view of colon.

rates, we can feel as if we are flying through the cylindrical closed space. In clinical applications doctors are expected to find symptoms of diseases such as polyps, tumors and inflammations.

Figure 4 illustrates effects of changes in the opacity table using one of such scenes of the colon wall. Here a typical polyp exists, but its apparent shape seriously varies according to the values of the opacity table of the VolR algorithm employed here. Thus we should be careful enough concerning what we are seeing in VolR images.

4.2. Example 2: The inside view of the lung

Let us proceed to the scenery of the lung. Figure 5 presents two scenes observed from the viewpoint located inside the lung. Parts of blood vessels, bronchus branches, ribs and chest wall are seen in the image. Small massive objects in the right image, which seem to

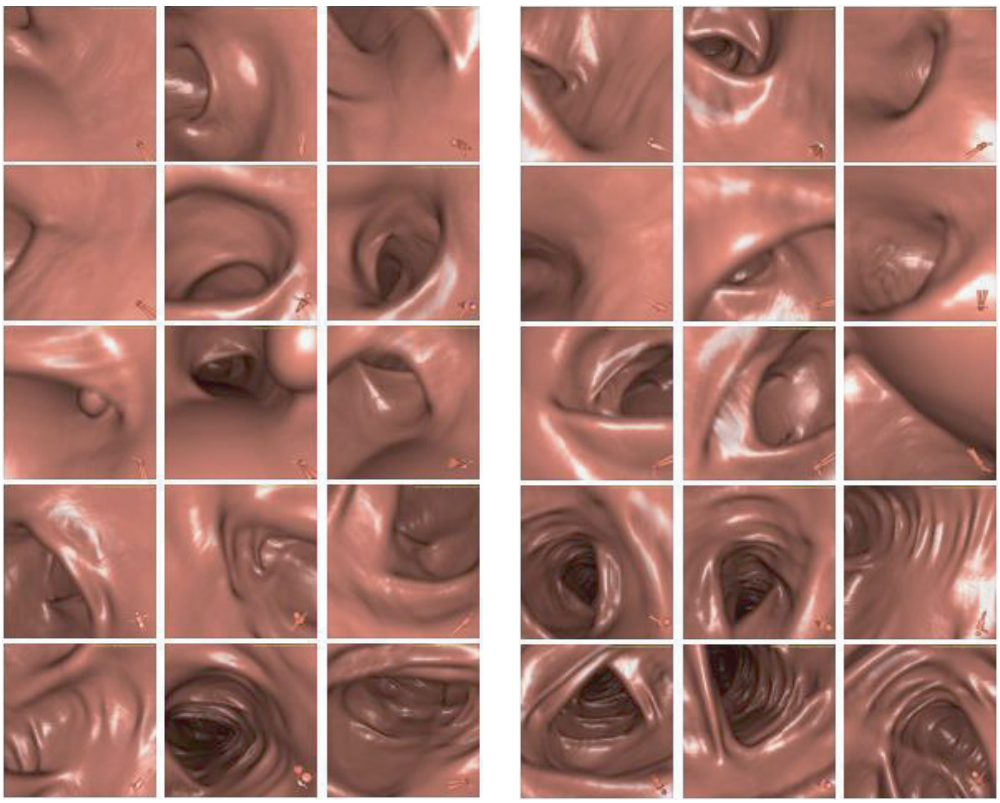

Fig. 3. Picture sequence showing inside views of colon (=views which will be seen in navigating inside the colon). The viewpoint was moved along the centerline of the case 2 in Fig. 2 from the bottom (the upper left of the figure) to the top (the lower right of the figure). Each picture shows the view in looking ahead in the tangential direction of the centerline at the sample point selected at even intervals (approximately 6 cm on the real body) on the path.

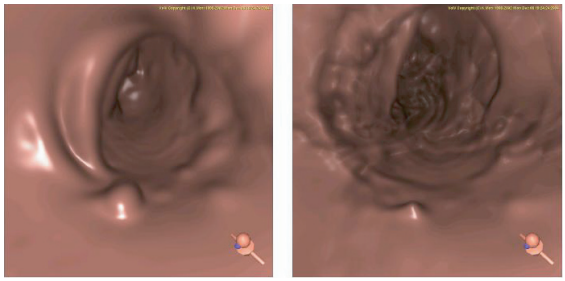

Fig. 4. Effect of change in the opacity table (1). The viewpoint and the view direction are the same for two pictures.

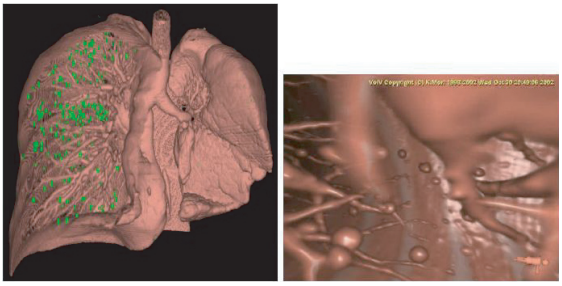

Fig. 5. Scenery of the lung.

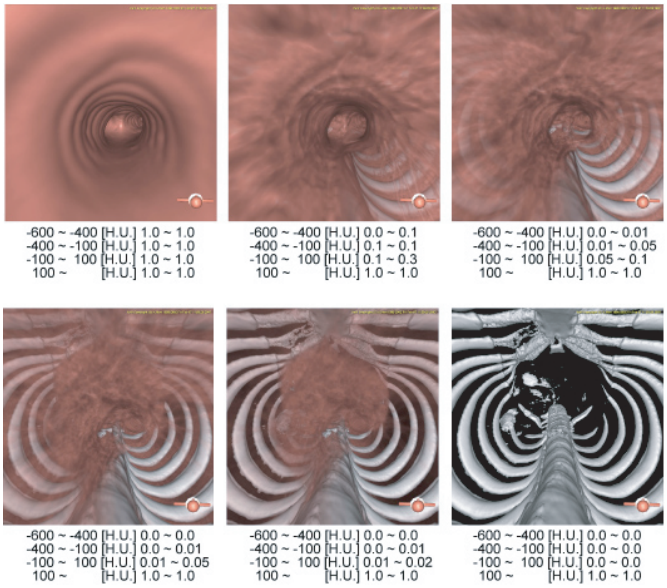

Fig. 6. Effect of change in the opacity table (2). H.U. means the Houndsfield Unit used for the density values in CT images. Numerals under the each image show opacity values used in rendering by VolR.

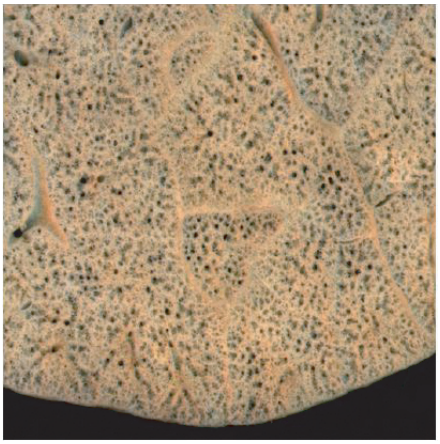

Fig. 7. Piece of the inflated fixed lung specimen.

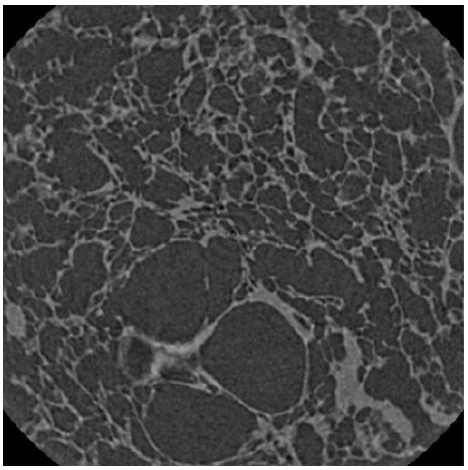

Fig. 8. Example of a slice of a μ-CT image of the lung specimen.

be floating in the air, are nodules suspected to be lung cancer. In this case more than 100 such small nodules were detected by a medical doctor. We can move around them, if needed for diagnosis. Those are marked by areas of green color at the corresponding locations in the left image. Such nodules are recognized as only small vague massive shadows scattered in the lung field of a slice of CT images. In these 3D images we can fly around among such many 3D nodules freely with examining details of shapes and calculating shape features. Even in this case, however, borders of nodules are not fixed decisively. They are only perceived visually in VolR images. Apparent shapes of nodules are very sensitive to values of the *opacity table* employed here (Fig. 6) (KUSANAGI *et al*., 2003; MEKADA *et al*., 2003).

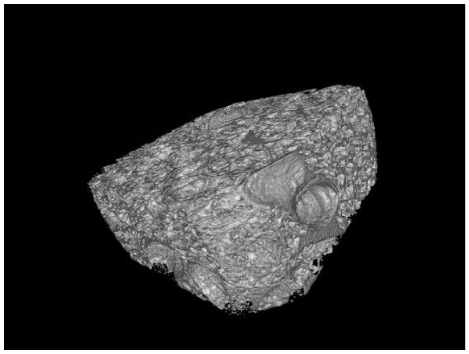

Fig. 9. Image of the whole sample specimen produced with volume rendering.

4.3. Example 3: Microstructure of lung tissue

The third example is the visualization of microstructure of the tissue of the lung. Source data was obtained by scanning a piece of an inflated fixed lung with micro CT scanner. Its spatial resolution is 0.2 μm approximately. Let us omit here detailed explanation of medical or anatomical contents of the structure. We would like to notice that the sample was made after a piece of an anatomical sample was dried. Therefore the structure seen here is a kind of skeleton structure of the architecture in living organ. However the approximated shape was preserved because the sample was filled with air after it was extracted and then dried (GROSKIN, 1993). The whole of the piece of the sample is shown in Fig. 7. Figure 8 shows an example of a slice of the CT image, and Fig. 9 is a VolR image of the whole of the sample. The real size is about 5 mm^3.

Let us show in Fig. 10 a VolR image with the viewpoint inside the piece of the sample used here. We can see the sophisticated architecture of parenchyma of the human lung, peripheral structure of thin bronchial branches, alveolar duct, alveolus etc. Basic units forming the lung architecture are the alveolus and the alveolar ducts. The number of alveolus is a key determinant of the lung architecture, and has been counted in various ways (OCHS *et al*., 2004). In this sample, however, individual alveolus is expected to be observed directly, because the mean size of a single alveolus was about 4.2×10^6 μm^3 (OCHS *et al*., 2004). The total number of alveoli was estimated as 480 million according to (OCHS *et al*., 2004). This value was derived by applying classical stereology to 2D sections observed by light microscope. Apart from medical or anatomical meanings, we can see complicated 3D network architecture. By shifting the viewpoint a little we see different views of this architecture. In the case of Fig. 10, the viewpoint is considered to be located inside a peripheral bronchus branch (left), and in the peripheral vein (right).

Shape features characterizing this architecture have not been proposed, nor been measured. In (OCHS *et al*., 2004), the Euler number of this architecture was estimated only by stereological method. In (MATSUBARA *et al*., 2003, 2004), the method proposed in (TORIWAKI and YONEKURA, 2002a, b) was applied to calculate 3D digital Euler number and the connectivity index from a 3D binary picture obtained by the threshold from the 3D gray

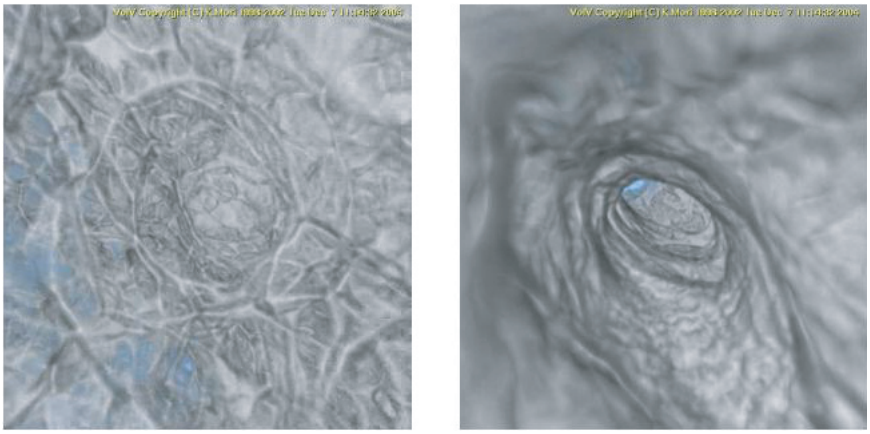

Fig. 10. Images produced with the volume rendering. The viewpoint seems to be located in a peripheral bronchus branch (left), and in the peripheral vein (right).

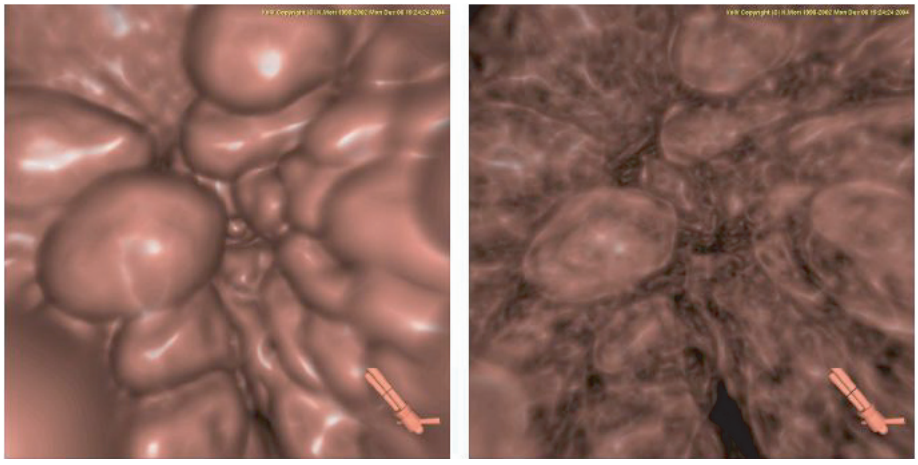

Fig. 11. Effect of change in the opacity table for the same material as Fig. 9, and 10.

tone image. Apparently similar structure is found in bone, although the size is larger than this (PARFITT *et al*., 1983; KINNEY and LADD, 1995; MAJUMDAR *et al*., 1995; SAHA and CHAUDHURI 1996; KINNEY *et al*., 1998; WEHRLI *et al*., 2000, 2001, 2003).

We should be careful, however, to interpret this image again, because the same problem as was described before occurs here, too. For example, Fig. 11 shows two VolR images of this sample from the same viewpoint and the same direction. Only the opacity tables are different among them. <Which is true?> is the reasonable question. Perhaps, they provide information of the shapes of 3D equi-density surface at the different level of

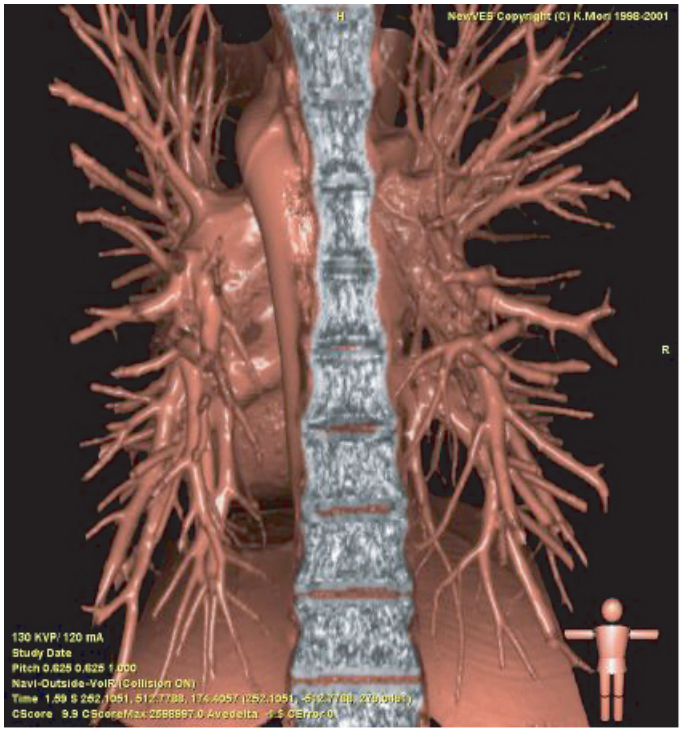

Fig. 12. Tree structure in the human body (back view of the body).

density values. Still we could have recognized some of individual alveoli by computer (SATO *et al*., 2004).

4.4. Example 4: Tree structure in the human body

Let us present several views of the tree structure in the human body. Figure 12 shows the bronchus tree and vessels extending from the hilum toward the peripheral of the lung. The gray column at the center of the image is the spine. The next image (Fig. 13) is vessels in the lung extracted automatically by the image analysis procedure and then were classified into arteries and veins by the medical specialist (TANAKA *et al*., 2004).

Strictly speaking, vessels and arteries in the lung are connected by capillary, but the present CT systems cannot record figures of the capillary. Thus vessels and bronchus branches are observed as the tree structures in CT images. Anatomical names are also given to individual branches regarding them as parts of tree structure.

4.5. Example 5: Abdominal organs

Finally let us show the outside views of major abdominal organs in Fig. 14. Since all organs in this figure were again extracted by pattern recognition by computer, their forms are not always exact, but important errors have not been found here (KITASAKA *et al*.,

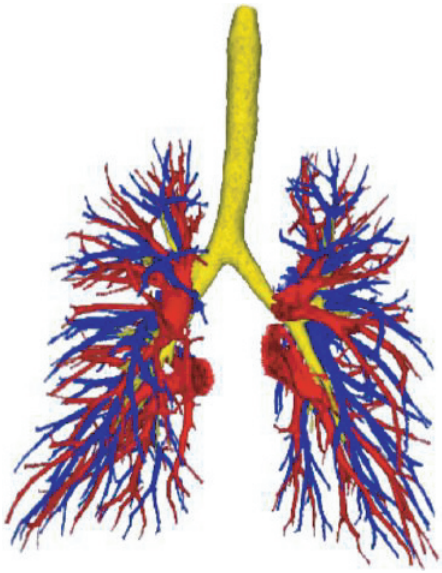

Fig. 13. Trachea, bronchus, and vessels in the lung.

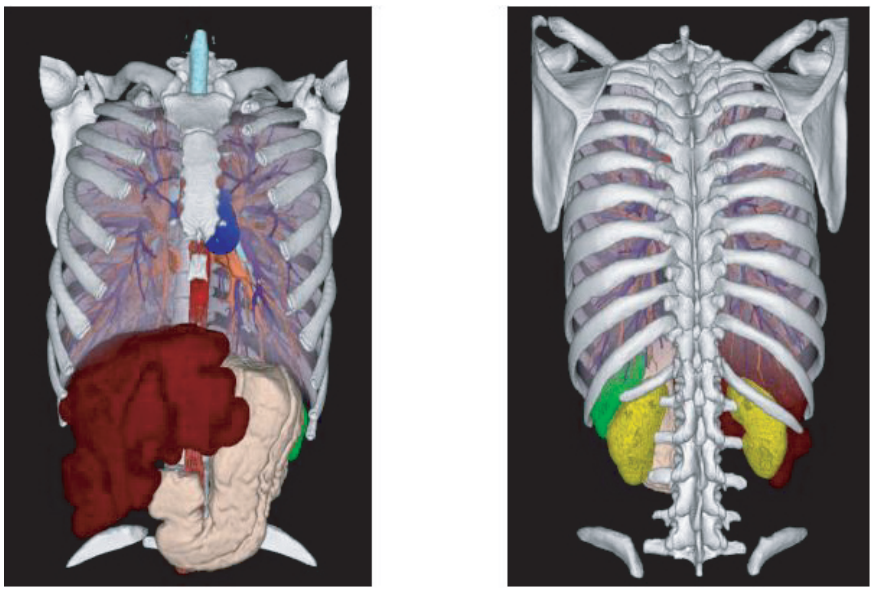

Fig. 14. Abdominal organs. Brown red: liver. Yellow: kidney. Green: spleen. Pink: lung and stomach. Light gray: bone.

2005). Anyway, we can never see such forms in living human body without X-ray CT images. However, we have not succeeded in deriving reasonable way of mathematical expressions for these forms.

5. Conclusion

In this article, the author briefly reviews methods to visualize forms of human organs and tissues as examples of forms found in natural things. By the great progress in recent imaging technologies we can obtain 3D digital images of parts of human body with the spatial resolution of 10 mm~10 μm. Once we have stored digitized data from scanning devices, we can reconstruct the individual human body (virtualized human body VHB) in computer. By visualizing VHB, we can see various forms existing in the human body. Furthermore we can move around or fly through inside the human body interactively.

The article presented several examples of images showing scenes inside the human body. All of them are characterized by that the viewpoint was set inside the body. However theoretical (or mathematical) analysis of those forms still remains unsolved for future problems. For instance, simple mathematical expressions for the form of colon have not been known. Shape features have not been reported for the complicated spatial architecture of the lung tissue. We expect that the science on form will contribute much to solving these problems in the near future.

The authors deeply thank all people listed below for their assistance. For providing CT images and for valuable discussion from medical viewpoints: Makoto Hashizume, MD, Kyushu University, Hiroshi Natori, MD, Sapporo Medical College, Masaki Mori, MD, Sapporo Kousei Hospital, Hirotsugu Takabatake, MD, Minami-Sanjo Hospital.

For producing VolR images included in the article and for significant collaboration: Kensaku Mori, Ph.D., Nagoya University, Yoshito Mekada, Ph.D., Chukyo University, Yuichiro Hayashi, Ph.D., Nagoya University, Takayuki Kitasaka, Ph.D., Nagoya University.

This research was partially supported by the Grant-in-Aid for Scientific Research from the Ministry of Education, Science and Culture, and the Grant-in-Aid for Cancer Research from the Ministry of Health and Welfare and Labor, and Grant-in-Aid for Private University High-tech. Research Center from the Ministry of Education, Science and Culture.

REFERENCES

BANKMAN, I. N. (ed.) (2000) *Handbook of Medical Imaging*, Academic Press.

DUCHMAN, A. H. (2003) *Atlas of Virtual Colonoscopy*, Springer-Verlag.

GROSKIN, S. A. (1993) *Heitzman's the Lung—Radiologic-Pathologic Correlations*, Mosby, St. Louis, U.S.A.

HAYASHI, Y., MORI, K., HASEGAWA, J., SUENAGA, Y. and TORIWAKI, J. (2003a) A method for detecting undisplayed regions in virtual colonoscopy and its application to quantitative evaluation of fly-through methods, *Academic Radiology*, **10**, 1380–1391.

HAYASHI, Y., MORI, K., HASEGAWA, J., SUENAGA, Y. and TORIWAKI, J. (2003b) Quantitative evaluation of observation methods in virtual endoscopy based on the rate of undisplayed region, in *Proc. of SPIE, Medical Imaging 2003, Physiology and Function: Methods, Systems, and Applications*, pp. 69–79.

HERMAN, G. T. (1998) *Geometry of Digital Spaces*, Birkhauser, Boston.

KINNEY, J. H. and LADD, A. J. (1998) The relationship between three-dimensional connectivity and the elastic properties of trabecular bone, *J. Bone Mineral Res.*, **13**, 839–845.

KINNEY, J. H., LANE, N. E. and HAUPT, D. L. (1995) In vivo, three-dimensional microscopy of rabecular bone,

J. Bone Mineral Res., **10**, 264–270.

KITAOLA, H., TAMURA, S. and TAKAKI, R. (2000) A three-dimensional model of the human pulmonary acinus, *J. Appl. Physiol.* **88**, 2260–2268.

KITASAKA, T., MORI, K., HAYASHI, Y., SUENAGA, Y., HASHIZUME, M. and TORIWAKI, J. (2004) Virtual pneumoperitoneum for generating virtual laparoscopic views based on volumetric deformation, in *7th International Conference on Medical Image Computing and Computer Assisted Intervention (MICCAI 2004.9), Saint-Malo, France, September, 26–29, 2004, Proceedings, Part II, LNCS 3217* (eds. C. Barillot, D. R. Haynor and P. Hwllier), pp. 559–567.

KITASAKA, T., OGAWA, H., YOKOYAMA, K., MORI, K., MEKADA, Y., HASEGAWA, J., SUENAGA, Y. and TORIWAKI, J. (2005) Automated extraction of abdominal organs from uncontrasted 3D abdominal X-ray CT images based on anatomical knowledge, *Journal of the Computer Aided Diagnosis of Medical Images*, **9**, 1–14.

KUSANAGI, T., MEKADA, Y., TORIWAKI, J., HASEGAWA, J., MORI, M. and NATORI, H. (2003) Correspondence of lung nodules in sequential chest CT images for quantification of the curative effect, *Proc. of CARS2003*, 983–989.

LEVOY, M. (1988) Volume rendering, display of surfaces from volume data, *IEEE Computer Graphics and Applications*, **8**, 29–37.

MAJUMDAR, S., NEWITT, D., JERGAS, M., GIES, A., CHIU, E., OSMAN, D., KELTNER, J., KEYAK, J. and GENANT, H. (1995) Evaluation of technical factors affecting the quantification of trabecular bone structure using magnetic resonance imaging, *Bone*, **17**, 417–430.

MATSUBARA, A., KITASAKA, T., MORI, K., SUENAGA, Y., TORIWAKI, J. and TABATAKE, H. (2003) A preliminary study on micro structure analysis of lung tissue (2), in *Paper of Professional Group, Institute of Electronics, Information and Communications Engineers, Japan*, PRMU2003-303, Vol. 103, No. 738, pp. 113–118.

MATSUBARA, A., KITASAKA, T., MORI, K., SUENAGA, Y. and TORIWAKI, J. (2004) A study on topological feature values of 3-D digital images—toward micor structure analysis of lung tissue—, in *Paper of Professional Group, Institute of Electronics, Information and Communications Engineers, Japan*, PRMU2003-303, Vol. 103, No. 738, pp. 113–118.

MEKADA, Y., KUSANAGI, T., HAYASE, Y., MORI, K., TORIWAKI, J., HASEGAWA, J., MORI, K. and NATORI, H. (2003) Detection of small nodules from 3D chest X-ray CT images based on shape features, in *Proc. of CARS2003*, pp. 971–976.

MORI, K., HASEGAWA, J. and TORIWAKI, J. (1994) A method to extract pipe structured components in three dimensional medical images and simulation of bronchus endscope images, in *Proc. of Conference on Three Dimensional Digital Images '94*, pp. 269–274.

MORI, K., SUENAGA, Y. and TORIWAKI, J. (2003) Fast software-based volume rendering using multimedia instructions on PC platforms and its application to virtual endoscopy, in *Proc. of SPIE, Medical Imaging 2003, Physiology and Function: Methods, Systems, and Applications*, pp. 111–122.

MORRISON, P. (1982) *P. Morrison and the Office of Charles and Ray Eames: Powers of Ten, about the Relative Size of Things in the Universe*, W. H. Freeman and Company, San Francisco.

OCHS, M., NYENGAARD, J. R., JUNG, A., KNUDESEN, L., VOIGT, M., WAHLERS, T., RICHITER, J. and GONDERSEN, H. J. G. (2004) The number of alveoli in the human lung, *Am. J. Respir Grit Care Med.*, **169**, 120–124.

ODA, M., KITASAKA, T., MORI, K. and SUENAGA, Y. (2004) Development of computer aided diagnosis system for colorectal cancer based on navigation diagnosis, in *Paper of Professional Group, Institute of Electronics, Information and Communications Engineers, Japan*, PRMU2004-18, MI2004-18, MI, Vol. 104, No. 91, pp. 35–40.

PARFITT, A. M., MATHEWS, C. H. E., VILLANUEVA, A. R., KLEEREKOPER, M., FRAME, B. and RAO, D. S. (1983) Relationships between surface, volume, and thickness of iliac trabecular bone in aging and in osteoporosis, Implications for microanatomic and cellular mechanisms of bone loss, *J. Clinical Invest*, **72**, 1396–1409.

ROGALLA, P., TERWISSCHA, J., SCHELTINGA, van and HAMM, B. (eds.) (2000) *Virtual Endoscopy and Related 3D Techniques*, Springer, Heidelberg, Germany.

SAHA, P. K. and CHAUDHURI, B. B. (1996) 3D digital topology under binary transformation with applications, *Comput. Vision Image Underatand.*, **63**, 418–429.

SAITO, T. and TORIWAKI, J. (1994) New algorithms for n-dimensional Euclidean distance transformation, *Pattern Recognition*, **27**, 1551–1565.

SAITO, T. and TORIWAKI, J. (1995) A sequential thinning algorithm or three dimensional digital pictures using

the Euclidean distance transformation, in *Proc. 9th SCIA (Scandinavian Conf. on Image Analysis)*, pp. 507–516.

SATO, Y., NAGAO, J., KITASAKA, T., MORI, K., SUENAGA, Y., TORIWAKI, J. and TAKABATAKE, H. (2004) Extraction of pulmonary alveoli from Micro CT image of lung tissue, in *Paper of Professional Group, Institute of Electronics, Information and Communications Engineers, Japan*, PRMU2004-9, MI2004-9, WIT2004-9, MI, Vol. 104, No. 90, pp. 49–54.

TANAKA, T., MEKADA, Y., MURASE, H., HASEGAWA, J., TORIWAKI, J., and OTSUJI, H. (2004) Automated classification of pulmonary artery and vein from chest X-ray CT images based on their spatial arrangement features, in *Proc. of the Sym. on Media and Image Recognition and Understanding 2004 (MIRU2004)*, Vol. I, pp. (I)15–20.

TORIWAKI, J. (1997) Virtualized human body and navigation diagnosis, *BME (Journal of Japanese Society for Medical and Biological Engineering)*, **11**, 8, 24–35 (in Japanese).

TORIWAKI, J. (2004a) Navigation observation with interactive operation of the viewpoint inside an object, Technical Report No. 2003-2-01, School of Computer and Cognitive Sciences, Chukyo University, Toyota, Japan.

TORIWAKI, J. (2004b) The front of radiation imaging technique (8): Navigation observation—observing objects with the free inside viewpoint and medical applications, *ISOTOPES*, **53**, 331–342.

TORIWAKI, J. (2002c) *Three-dimensional Image Processing*, Shokodo (in Japanese).

TORIWAKI, J. and MORI, K. (2001) Distance transformation and skeletonization of 3D pictures and their applications to medical images, in *Digital and Image Geometry, Advanced Lectures, LNCS (Lecture Notes in Computer Science)* (eds. G. Bertrand, A. Imiya and R. Klette), pp. 2243, pp. 412–428, Springer-Verlag.

TORIWAKI, J. and YONEKURA, T. (2002a) Euler number and connectivity indexes of a three-dimensional digital picture, *FORMA*, **17**,173–209.

TORIWAKI, J. and YONEKURA, T. (2002b) Local patterns and connectivity indexes in a three dimensional digital picture, *FORMA*, **17**, 275–291.

VINING, D. J. (2003) Virtural colonosocopy: The inside story, in *Atlas of Virtual Colooscopy* (ed. V. H. Dachman), pp. 3–4, Springer-Verlag, N.Y.

VINING, D. J., PADHANI, A. R., WOOD, S., ESERHOUNI, E. A., FISHMAN, E. K. and KUHLMENN, J. E. (1993) Virtual bronchoscopy: a new perspective for viewing the tracheobronchial tree, *Radiology*, **189**(P), Nov.

WATT, A. and POLICARPO, F. (1998) *The Computer Image*, Addison-Wesley.

WEHRLI, F. W., SAHA, P. K., GONBERG, B. R. and SONG, H. K. (2000) noninvasive assessment of bone architecture by magnetic resonance micro-imaging-based virtual bone biopsy, *Proc. of the IEEE*, **91**, 1520–1542 (2003.10); *J. Appl. Phsiol.*, **88**, 2260–2268 (2000).

WEHRLI, F. W., GONBERG, B. R., SAHA, P. K., SONG, H. K., HWANG, S. N. and SNVDER, P. J. (2001) Digital topological analysis of in vivo magnetic resonance microimages of trabecular bone reveals structural implications of osteoporosis, *J. Bone Mineral Res.*, **16**, 1520–1531.

WEHRLI, F. W., SAHA, P. K., GONBERG, B. R. and SONG, H. K. (2003) Noninvasive assessment of bone architecture by magnetic resonance micro-imaging-based virtual bone biopsy, *Proc. of the IEEE*, **91**, 1520–1542.